POLYPUBLIE
Polytechnique Montréal

POLYTECHNIQUE
MONTRÉAL

UNIVERSITÉ
D'INGÉNIERIE

Titre: Title:	Recovery of gold from e-waste via food waste byproducts
Auteurs: Authors:	Teresa Cecchi, Zhaojing Gao, Christophe Clément, Anthony Camus, Andrew Karim, Olivier Girard, & Clara Santato
Date:	2023
Type:	Article de revue / Article
Référence: Citation:	Cecchi, T., Gao, Z., Clément, C., Camus, A., Karim, A., Girard, O., & Santato, C. (2023). Recovery of gold from e-waste via food waste byproducts. Nanotechnology, 34(6), 065203 (8 pages). https://doi.org/10.1088/1361-6528/ac9ec6

Document en libre accès dans PolyPublie
Open Access document in PolyPublie

Document publié chez l'éditeur officiel
Document issued by the official publisher

PAPER • OPEN ACCESS

Recovery of gold from e-waste via food waste byproducts

View the article online for updates and enhancements.

Recovery of gold from e-waste via food waste byproducts

Teresa Cecchi[1,*] ⓘ**, Zhaojing Gao**[2]**, Christophe Clement**[2]**,
Anthony Camus**[2] ⓘ**, Andrew Karim**[2]**, Olivier Girard**[3] **and Clara Santato**[2,*] ⓘ

[1] Istituto Tecnico Tecnologico (ITT), G. and M. Montani, I–63900, Fermo, Italy
[2] Engineering Physics, Polytechnique Montreal, H3T 1J4, Montreal, QC, Canada
[3] Centre For Characterization And Microscopy Of Materials (CM)2, Polytechnique Montreal, H3T 1J4, Montreal, QC, Canada

E-mail: cecchi.teresa@istitutomontani.edu.it and clara.santato@polymtl.ca

CrossMark

Abstract
Global materials' and energy constraints and environmental issues call for a holistic approach to waste upcycling. We propose a chemically rational, cost-effective and environmentally friendly recovery of non-leaching gold from e-waste using aqueous chemistry with hydrogen peroxide, an environmentally benign oxidant, and lactic acid, a food chain byproduct. The oxidation of the base metals enables the release of gold in its metallic state in the form of flakes subsequently separated via filtration. Our main byproduct is a precursor of Cu_2O, a relevant metal oxide for solar energy conversion applications. The recovered gold was characterized by scanning electron microscopy, energy dispersive spectroscopy and x-ray photoelectron spectroscopy to gain insight into the morphology of the flakes and their chemical composition. Furthermore, recovered gold was used to successfully fabricate the source and drain electrodes in organic field-effect transistors.

Supplementary material for this article is available online

(Some figures may appear in colour only in the online journal)

1. Introduction

The increasing demand for electronics along with planned obsolescence contribute to the dramatic accumulation of waste electrical and electronic equipment (WEEE or e-waste), at the global level [1]. E-waste comprises base metals (e.g. Cu, Ni, Pb, Zn, Fe, Sn, Al), precious metals (e.g. Au, Pd, Pt), specialty metals (e.g. In, Ga, Se, Sb, Te, Ta, rare Earth elements), and toxic metals (e.g. Hg, Cr, Cd) [2–8].

Printed circuit boards (PCBs) are the core of most electronics. Even if they contribute to only 6% of the weight of e-waste, they are a key source of valuable metals, [9] whose concentration can be several times higher than in their primary ore minerals. The recovery of such valuable metals is needed to maintain their supply chain and reduce the effect of mining on human health and the environment [3, 4, 10]. Among valuable metals, Au plays the role of the 'paying metal' [10, 11].

A complex challenge such as precious metals' recovery is expected to require a number of different solutions. Among them are the pyrometalluyrgical and hydrometallurgical ones. The suitability of a solution over another one is dictated by a number of factors, such as local specific needs and constraints [12]. Hydrometallurgy is an important route to recover Au. Here, an oxidation step is typically used to dissolve Au (and metals more oxidizable than gold) and a subsequent reduction step selectively brings Au ions to metallic Au.

* Authors to whom any correspondence should be addressed.

Cyanide and aqua regia (HNO_3:HCl in a molar ratio 1:3) are often used in Au oxidation, even if the toxicity of the former and the corrosiveness of the latter endanger workers and the environment [13].

The classical hydrometallurgical gold recovery strategy is not rational from the chemical point of view, for at least three reasons: (i) it requires harsh chemical treatment of e-waste, harmful to workers and the environment, to firstly oxidize and subsequently reduce gold; (ii) it results in large amounts of wastewater; (iii) it triggers a downcycling of gold whose purity would be certainly lower after the dissolution and reductive recovery, compared to the original purity in the e-waste.

Chemical schemes avoiding gold oxidation have been already reported in the literature: an hydrochloric acid/iron (III) mixture [14], various persulfate solutions [15–18], $CuCl_2$ acidic solutions [19], a methane sulfonic acid/H_2O_2 mixture [20] brought to the selective oxidation of base metals with Au release in its original metallic state.

Even if metal ions in their highest oxidation state, such as Cu^{2+} or Fe^{3+}, proved to be effective in base metal oxidation leading to gold removal, they represent an additional disposal problem because they remain in the reaction mixture; similarly, persulfate-based oxidation suffers from the sulfate leftover in the reaction mixture.

H_2O_2 is widely used in hydrometallurgical processes because it is a safe and effective oxidant [21]. It oxidizes base metals, e.g. Cu, according to the following reaction:

$$H_2O_2 + 2H^+ + Cu \rightarrow 2H_2O + Cu^{2+}. \tag{1}$$
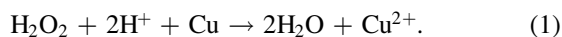
The non-toxicity of the reduction product (water) is noteworthy from the environmental point of view.

The acidification of the reaction medium through upcycling of waste chemicals would be of the highest interest, here, for environmental and economic viability considerations.

Lactic acid (LA) is a biobased platform chemical that can be obtained from food waste upcycling [22]. Commercial LA is usually produced by the bacterial fermentation of carbohydrates by homofermentative organisms belonging to the genus Lactobacillus and Bacillus. In order to limit the land use share for its production, a wide range of high sugar-containing food waste such as coffee mucilage, corn cobs, corn stalks, rice bran, barley, wheat bran, brewer's spent grains, kitchen waste, pineapple and grape waste, soybean vinasse, *Curcuma longa* biomass, and yoghurt waste have been explored as alternative feedstocks for fermentative LA production [23]. Whey, whose discharge is a major pollution problem for the dairy industry, is a potent and suitable raw material for LA production in a real 'gutter to gold' approach [24].

LA is also known to complex metal ions, thereby providing an extra driving force for base metal leaching [25]. At the same time, Fenton-like reactions catalyzed by metals such as Cu^{2+} and Ni^{2+} and leading to the *in situ* generation of hydroxyl radical (HO·) capable to oxidize base metals cannot be excluded [26–28].

Here, we report on an environmentally benign and low-cost route that makes use of a green oxidant (H_2O_2) and an organic acid from food waste upcycling (LA) to achieve base metals oxidation and peeling of metallic Au from random access memory (RAM) PCB e-waste. We characterized the morphology and elemental composition in pristine and peeled Au by scanning electron microscopy (SEM) and energy dispersive spectroscopy (EDS). Afterwards, we used the recovered Au to fabricate by e-beam evaporation photolithographycally patterned metal contacts on SiO_2/Si substrates. We performed chemical surface analysis by x-ray photoelectron spectroscopy (XPS) on peeled gold and e-beam evaporated metal contacts from peeled gold. Such contacts were succesfully employed as source and drain elctrodes in field-effect transistors (FETs) making use of the well-investigated organic semiconducting polymer poly(3-hexylthiophene-2,5-diyl) (P3HT) as transistor channel material. The contacts were characterized for their morphological properties by atomic force microscopy (AFM), to shed light onto device performance.

2. Experimental

2.1. Materials and reagents

RAMs were taken from PCBs removed from dismissed PCs. A guillotine was used to cut RAM. L-LA (2-hydroxy-propionic acid) 90 w/w% was obtained from Carlo Erba (density: 1.20 g ml^{-1}, 13 .318 M). Hydrogen peroxide 35% w/w% (density: 1.130 g ml^{-1}, 11 .627 M) was obtained from Italchimici Group. Ultrapure water (18.2 MΩ.cm at 25 °C) was produced via a Millipore Simplicity® UV system.

The RAM boards used for systematic experiments described in table 1 were (i) ELIXIR 512 MB DDR-400 MHz-CL3 PC3200U-30330 and (ii) S3 + PC3200/DDR400 512 MB.

The RAM boards used in the subsequent massive peeling of gold for the FET fabrication were (i) ELIXIR 512 MB DDR-400 MHz-CL3 PC3200U-30330; (ii) S3 + PC3200/DDR400 512 MB; (iii) AE 512 MB 1Rx8 PC2–4200U-444–11 AET660UD00–370A98Z A1K62517 Pb free; (iv) NANYA NT 128D64S88A0G-7K, 128 MB, DDR 266 MHz-CL2, PC2100U-20330, 0206.A1032; (v) I HYS64-T64000HU-3S-A A2E62621 512 MB 1Rx8 PC2–5300U-555–12-D0 Pb free; (vi) I HYS64T64000HU-3.7-A 512 MB, 1Rx8 PC2–4200U-444–11-A1 Pb free; (vii) HYNIX 1 GB 2Rx8 PC2–5300U-555–12 HYMP512U64CP8-Y5 AB-C; (viii) NANYA NT 512D64S5HB1G- 5T 512 MB, DDR 400 MHz-CL3, PC3200U-30330; (ix) TEAM Group Inc. TVD32048M1333C9 2 GB DDR III 1333 MHz; (x) RAMAXEL 512 MB 1Rx8 PC2–5300DDU-555 LF. A mass of 2897.886 g of these RAM waste was guillotined to obtain 149.886 g of RAM edges that were subsequently treated according to the experimental condition A (table 1).

2.2. Systematic experiments for gold peeling

Experiments to shed light onto the effect of gold peeling conditions on the effectiveness of the process were carried out in triplicata in a 100 ml glass reaction vessel, under a fume hood. Known amounts of waste edges and reagents were mixed (table 1). Gold peeling was also monitored for different

Table 1. Systematic experiments with lactic acid (LA) and H_2O_2 mixtures in the experimental conditions indicated as *A*, *B*, *C*, *D*. We specified LA and H_2O_2 concentrations (*M*) in each mixture, gold peeling outcome (by eye, figure SM1), base metal amounts leached per gram of waste RAM (ELIXIR 512 MB DDR-400 MHz-CL3 PC3200U-30330 and S3 + PC3200/DDR400 512 MB) edges $(mg\ g)^{-1}$ by ICP OES and the relative standard deviation (RDS) of three specimens from one samples (%). In each case, the final volume was 20 ml and RAM edges were 5% (w/v) of the reagent solution.

	Experimental condition			
	A	*B*	*C*	*D*
C_{LA} (M)	6.0	3.0	2.0	1.0
C_{H2O2} (M)	6.0	3.0	2.0	1.0
complete peeling in 12 h	yes	yes	yes	no
Cu (mg g^{-1} RAM edges)	213.949	230.908	236.457	0.316
Ni (mg g^{-1} RAM edges)	16.405	17.268	17.112	1.251
Zn (mg g^{-1} RAM edges)	0.294	0.340	0.321	0.115
Pb (mg g^{-1} RAM edges)	0.050	0.063	0.072	0.003
Au (mg g^{-1} RAM edges)	0.002	0.002	0.002	0.001
Cu RSD (%)	0.9	1.6	1.4	1.2
Ni RSD (%)	1.5	1.2	1.1	0.9
Zn RSD (%)	1.3	1.5	1	0.9
Pb RSD (%)	1.2	1.6	1.7	0.9
Au RSD (%)	1.1	1.3	1.7	1.5

reaction times and temperatures (not shown). The Au flakes recovered were separated from the solution containing base metal ions via simple filtration, using a Gooch crucible. They were dried overnight at 180 °C and weighted to calculate the recovery rate. Filtrates were subsequently analyzed.

2.3. Spot test for gold in solution

The presence (or absence) of Au^{3+} in the base metal solutions was tested via a spot test, using a 20% (w/v) Sn^{2+} chloride in 15% (w/w) hydrochloric acid, based on the following reaction [29]:

$$3Sn^{2+} + 2Au^{3+} \rightarrow 3Sn^{4+} + 2Au. \qquad (2)$$
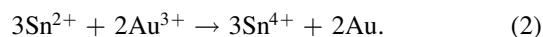
In presence of Au^{3+}, the newly formed metallic gold coalesces into colloidal dark particles with a wide range of sizes, resulting in light absorption throughout the whole optical spectrum [30].

2.4. Inductively Coupled Plasma Optical Emission Spectroscopy (ICP OES) and UV–vis spectrophotometry of base metal solutions

The filtrates were assessed in triplicata by ICP OES to determine the base metal ions concentrations via an optical emission spectrometer Perkin Elmer ICP Optima 8300. A blank correction was used. Base metal emission lines were 327.393 nm for Cu, 231.604 nm Ni, 206.200 nm for Zn, 220.353 nm for Pb, and 267.595 nm for Au. The UV–vis spectrophotometer used (a C-7200 a spectrophotometer, Peak Instruments Inc.).

2.5. Massive peeling of gold

The experimental condition *A* in table 1 was selected to peel gold from a mixture of RAM boards (as indicated in 2.1) for transistor fabrication.

2.6. SEM and EDS on pristine edges and peeled gold flakes

For SEM studies, we used a FEG JEOL 7600F microscope. The chemical analyses were carried out using a 80 mm^2 area SDD EDS X-Max (Oxford Instruments). Most of the images were taken at an accelerating voltage of 5 kV with a ET secondary electron detector. The chemical analyses were also done at 5 kV. Samples from RAM boards for systematic experiments (see materials and reagents) were considered for these studies on pristine cut edges and peeled Au. SEM observations were first carried out on peeled Au flakes and their thicknesses were found to be not less than a micron. Electron trajectories simulations were then made using CASINO [31] to find the proper accelerating voltages to use for surface and volume EDS chemical characterization, respectively 5 kV and 15 kV. The latter was identified as the highest SEM accelerating voltage for which the electron beam is entirely contained inside the thickness of the flake. 3 kV EDS analyses were also made for top surface investigations. Afterwards, analogous EDS analyses were carried out on the RAM edges to compare the chemical composition.

2.7. X-ray photoelectron spectroscopy (XPS)

XPS analysis was carried out under vacuum ($<10^{-9}$ Torr) conditions using VG ESCALAB 3 MKII, equipped with an Al K-alpha x-ray source (1486.6 eV). The XPS full survey spectrum was recorded from 0 to 1350 eV with a step size of 1 eV, dwell time of 100 ms and pass energy of 100 eV. The peak position in the XPS spectrum was referenced to C-C at 285.0 eV.

2.8. Microfabrication and transistor characterization

Gold flakes were rinsed with DI water and then collected using a system including an Erlenmeyer flask, a frit glass and a vacuum pump. The flakes were then dried in the oven at 60 °C for 3 h prior e-beam evaporation. Bottom-contact, bottom-gate transistors were fabricated on doped silicon substrates with a 200 nm thick silicon dioxide (SiO_2) gate dielectric. Source and drain electrodes were made of 5 nm thick Ti adhesion layer and 10 nm thick Au. The electrode width (*W*) was 2.5 cm and the interelectrode distance (*L*) was 10 μm. We measured the resistance of the recycled and commercial Au electrodes, In the former case, the average resistance was ca. 4×10^5 Ω, which corresponds to a resistivity of 2×10^{-3} Ω m. In the latter case, the average resistance was ca. 10 Ω, which corresponds to a resistivity of 5×10^{-8} Ω m.

2.9. Atomic force microscopy (AFM)

The morphology of source and drain electrodes from commercial and recycled gold was acquired at ambient conditions

(relative humidity between 30% and 50%) by AFM in tapping mode (Bruker AFM FAST SCAN ICON) using an Al-coated Si cantilever, radius of 10 nm, spring constant ca. 40 N m^{-1}.

2.10. Semiconducting film fabrication and transistor characterization

Thin films of regioregular poly(3-hexylthiophene-2,5-diyl) (RR P3HT) with molecular weight of 50–70 kDa, purchased from Rieke Metals, were deposited on pre-patterned source and drain SiO$_2$/Si substrates by spin coating (1500 rpm, 100 sec) from a 10 mg ml^{-1} solution in chlorobenzene, under N$_2$ atmosphere, after the solution was stirred at 50 °C overnight. Each device was thermally treated on a hotplate at 110 °C for 10 min.

Transistors were characterized at room temperature, in a house-made probe station, inside a N$_2$ glove box, using an Agilent B1500A semiconductor parameter analyzer.

3. Results and discussion

To shed light on the effect of reagents' concentrations, we performed a series of experiments, indicated as *A*, *B*, *C*, *D* in table 1. In each case, the H$_2$O$_2$/LA molar ratio was 1.

Figures 1(a) and (b) show, respectively, the waste RAM boards used for experiments described in table 1 and the corresponding cut edges. Lowering the reagent concentrations below 2.0 M prevents the efficient removal of base metals and the completeness of the gold peeling process. The ICP-OES analyses of the filtrates show that the presence of leached base metals is lower in experiment *D* (table 1). Be, Cd, Li, Mn, Mo, Sn, Tl concentrations in *all* filtrates were never above their limit of quantitation (not shown). Results in table 1 indicate that the RAM edges mainly contain Cu, Ni and Zn [11]. Ag, Al, As, B, Ba, Co, Cr, Fe, Sb, Se, Ti were never above 0.05 mg per g of waste RAM edge (not shown). Au was not significantly leached, as indicated by the results in table 1 and the negative spot tests.

Considering the wide range of different RAMs present in e-waste, to ensure the effectiveness of the process, we selected condition A for the subsequent massive peeling of gold because the high concentration of chemicals in A is expected to promote the advancement of the reaction through the increase of the reaction rate. Figure 1(c) illustrates the reaction mixture after 12 h, for the experimental condition A, while the recovered metallic gold can be observed in figure 1(d). Under this condition, the recovered metallic gold was 0.630 g; considering that the mass of RAM waste was 2897.886 g and that from this amount 149.886 g of RAM edges were obtained, the yield of recovered metallic gold was 0.42% relative to the mass of waste RAM edges or 0.02% relative to the total mass of waste RAM. Further, 90% of the RAM edges were completely peeled , (i.e. 10% were partially peeled). Complete peeling could be obtained via e.g. vigorour stirring.

The reaction mixture where H$_2$O$_2$/LA molar ratio was up to 1.4 proved to be as efficient as C$_{H2O2}$/C$_{LA}$ = 1 for gold peeling in 12 h, such that the C$_{H2O2}$/C$_{LA}$ ratio was not
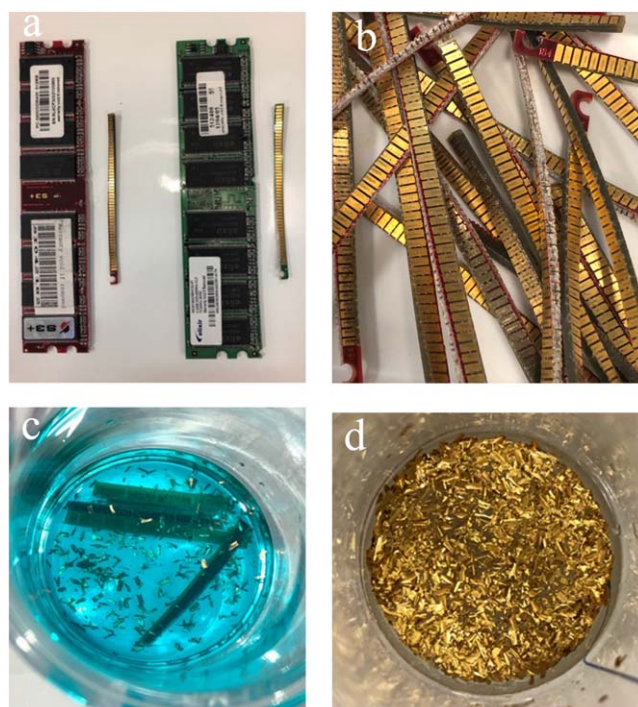

Figure 1. (a) Waste RAM boards used for experiments described in table 1 (ELIXIR 512 MB DDR-400 MHz-CL3 PC3200U-30330 and S3 + PC3200/DDR400 512 MB), (b) corresponding cut edges, (c) reaction mixture after 12 h, treatment for the experimental condition *A* in table 1, (d) recovered metallic Au.

increased beyond 1. Further, the decrease of the ratio to 0.6 did not enable complete gold peeling after 12 h.

Cupric lactate was the main constituent of the filtrate (figure SM2) [25]. This compound could be upcycled to synthesize Cu$_2$O-based photocatalysts [32, 33] or conducting inks based on LA-stabilized copper nanoparticles [34].

3.1. SEM and EDS

We characterized our pristine and peeled samples by SEM and EDS (figure 2 and figure SM3). In the former case, SEM images show that the surface of the edges features micrometric bumps and EDS indicates the presence of Au, Ni and Cu (besides C and O). In a small fraction of the investigated samples, we observed the presence of Zn, Mg and Si (about 10%, not shown). After peeling, samples are made of flakes with sizes in the millimetric range and the main element detected by EDS was Au (besides C and O). Ni, Cu and Na were observed in a small fraction on the investigated samples (about 10%, not shown).

All in all, EDS spectra indicate the effectiveness of the proposed H$_2$O$_2$/LA-based room temperature peeling treatment to remove metallic gold from RAM edges.

3.2. X-ray photoelectron spectroscopy (XPS)

Prior e-beam evaporation of peeled gold flakes to fabricate recycled Au metal contacts for OFETs, we characterized the surface chemical composition of the peeled flakes by XPS
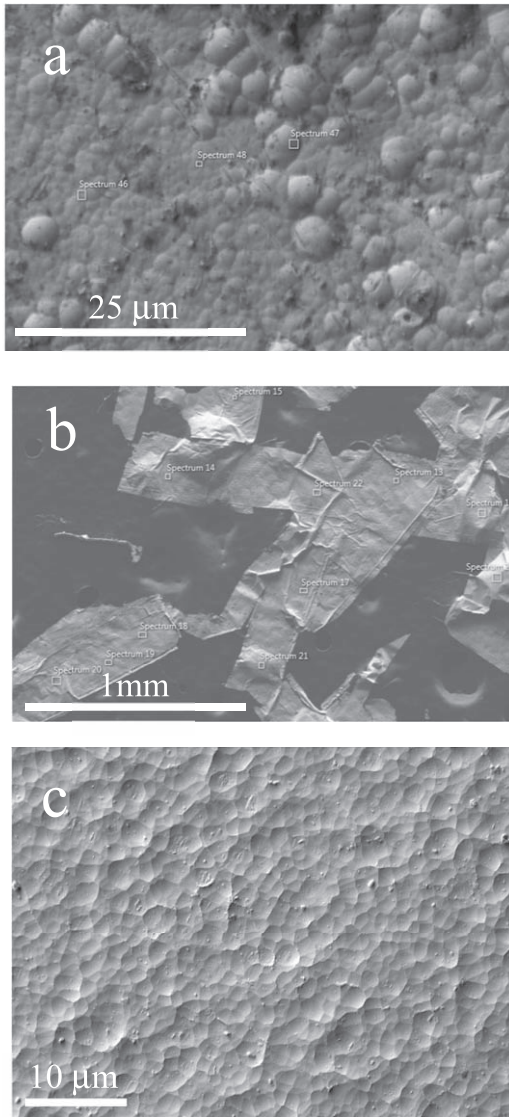
Figure 2. SEM images of (a) pristine RAM edges and (b) and (c) peeled flakes of Au removed from RAM edges.
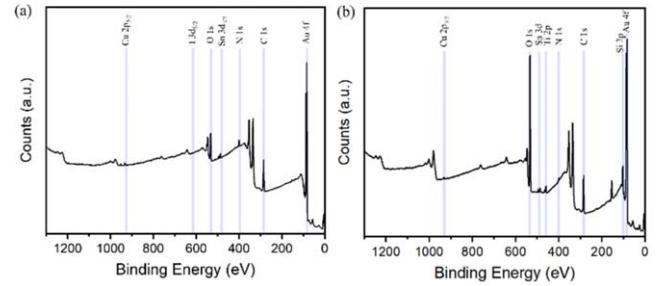

Figure 3. XPS survey spectra of (a) Au peeled flakes and (b) evaporated Au on silicon dioxide with titanium adhesion layer between silicon dioxide and gold.
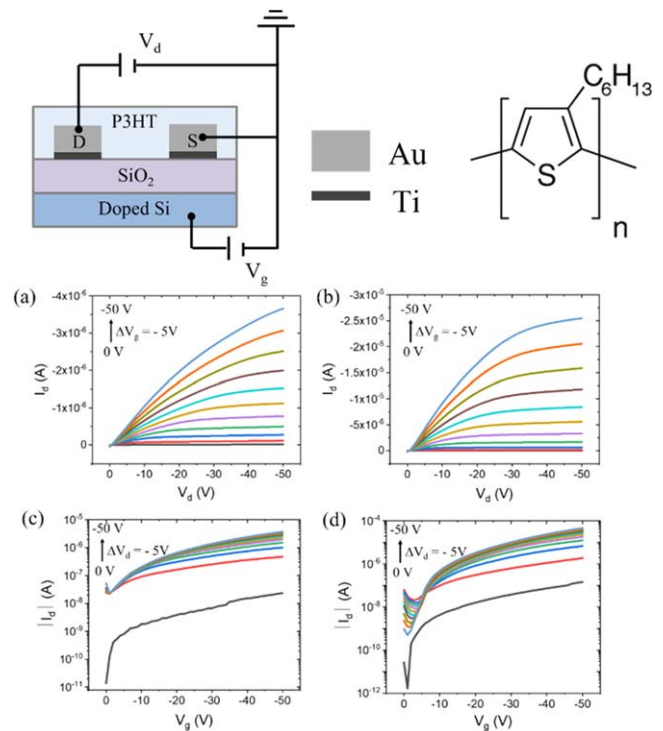

Figure 4. Output (a) and (b) and transfer (c) and (d) characteristics of P3HT field-effect transistors based on recycled (a) and (c) and commercial (b) and (d) Au source and drain electrodes. The scheme of the P3HT field-effect transistors and the molecular structure of the repeating unit in P3HT are also shown, respectively on top left and top right of the figure.

(figure 3, table SM1). The chemical species detected was mainly Au, besides C, O and N, with traces of Cu, Sn and I. Afterwards, an XPS characterization was carried out on source and drain electrodes e-beam evaporated from flakes of recovered gold. The chemical species detected was mainly Au, besides C and O, with traces of Cu and Sn. Ti and Si originating from the Ti adhesion layer located between Au and SiO_2 together with Si from SiO_2 were also detected.

3.3. Transistor characterization

After the morphological and chemical characterization of peeled gold, we fabricated field-effect transistors based on source and drain electrodes from commercial and peeled gold. The semiconducting channel material was P3HT, a well investigated organic electronic polymer. The output (drain-source current, I_{ds}, versus drain-source voltage, V_{ds}, for increasing values of the gate-source voltage, V_{gs}) and transfer

(I_{ds} versus V_{gs} for increasing values of V_{ds}) characteristics of the P3HT transistors show, as expected, that devices are p-type (holes are the majority carriers) and work in accumulation mode (figure 4) [35]. The hole mobility for transistors making use of commercial gold, as deduced from transfer characteristics at saturation was $(3.1 \pm 0.3) \times 10^{-4}$ cm^2/versus whereas it was $(6.3 \pm 0.8) \times 10^{-5}$ cm^2/versus for transistors making use of recycled gold. In linear conditions, the two values were $(1.4 \pm 0.1) \times 10^{-4}$ cm^2/versus and $(4.9 \pm 1.2) \times 10^{-5}$ cm^2/versus, respectively. A zoomed view of the outout characteristics in the low V_{ds} voltage region shows a linearity which reveals the ohmicity of the contacts (figure SM4). The threshold voltage is about -8 V for both

5.6 nm

Height Sensor　　　400.0 nm
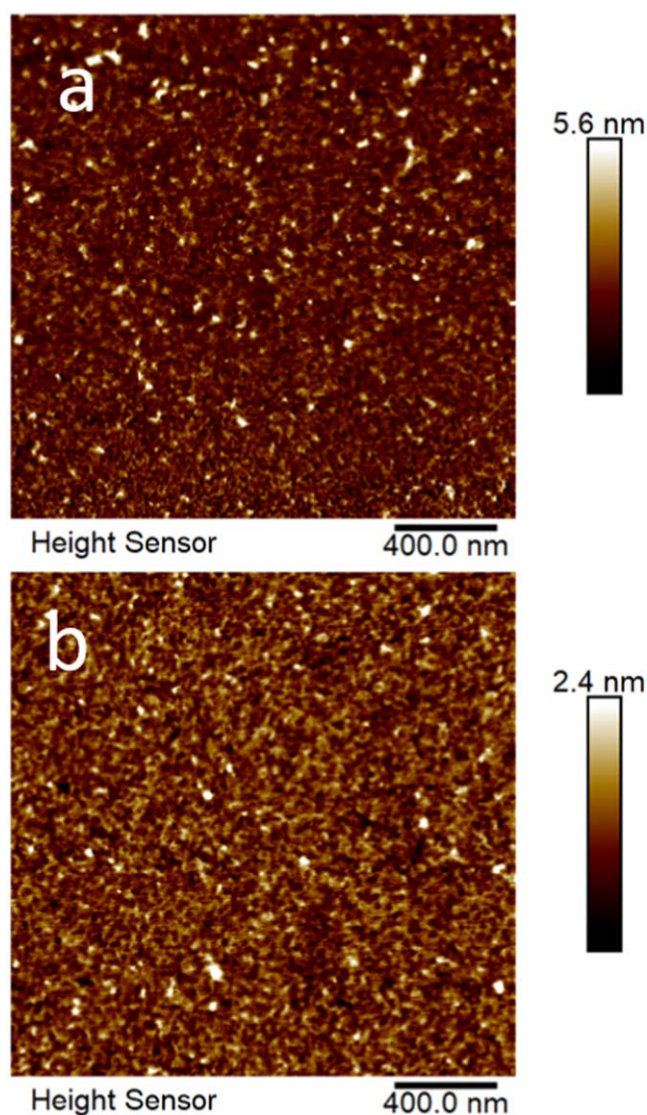
2.4 nm

Height Sensor　　　400.0 nm

Figure 5. Atomic force microscopy images of e-beam evaporated Au from (a) commercial and (b) recycled flakes.

types of transistors whereas the ON/OFF ratio (I_{ON}/I_{OFF} calculated from I_{ds} measured between $V_{gs} = -50$ V and $V_{gs} = 0$V at $V_{ds} = -50$ V) is ca. 10^3 and 10^2 for P3HT FET based on commercial and recycled gold, respectively.

3.4. Morphological characterization of evaporated gold films

AFM images of films evaporated from commercial and recycled gold showed similar morphologies (figure 5 and SM5), with grain-like structures. Commercial gold films feature a rougher topography, with rms roughness of about 0.7 nm. Recycled gold films are smoother, with rms roughness of about 0.4 nm.

It is worth mentioning that recycled gold films feature smaller grain-like structures than their commercial counterparts. This last observation could explain the higher resistance measured in recycled gold films as smaller grain-like structures imply an increased number of grain boundaries acting as resistances to transport [36–38].

4. Conclusions

Circular economy models encourage closing the loop of materials used in electronic devices. We have shown that this is possible for gold from e-waste that we recovered and recycled to fabricate source and drain electrodes of organic field-effect transistors. The contact resistance being higher in P3HT transistors making use of recycled gold with respect to their commercial gold counterparts, we are now optimizing the recovery process to increase the purity of the recovered gold.

To recover gold, we made use of an environmentally benign oxidant such as hydrogen peroxide and LA, obtainable from food waste. We wish to highlight the affordability of the process that could be adopted by low and medium income countries, too. We observed a selective removal of metallic gold with respect to base metals and the main byproduct of the base metals was copper lactate.

We are currently considering waste-based acids other than LA. In perspective, we plan to explore the use of copper lactate to synthesisze Cu_2O, a semiconducting photocatalyst to be applied in solar water splitting.

Acknowledgments

Data availability statement

All data that support the findings of this study are included within the article (and any supplementary files).

ORCID iDs

Teresa Cecchi ⓘ https://orcid.org/0000-0003-1940-864X
Anthony Camus ⓘ https://orcid.org/0000-0002-4405-388X
Clara Santato ⓘ https://orcid.org/0000-0001-6731-0538

References

[1] Vaccari M, Vinti G, Cesaro A, Belgiorno V, Salhofer S, Dias M I and Jandric A 2019 WEEE treatment in developing countries: Environmental pollution and health consequences —an overview *Int. J. Environ. Res. Public Health* **16** 9

[2] Schaeffer N, Passos H, Billard I, Papaiconomou N and Coutinho J A P 2018 Recovery of metals from waste electrical and electronic equipment (WEEE) using unconventional solvents based on ionic liquids *Crit. Rev. Environ. Sci. Technol.* **48** 859–922

[3] Batnasan A, Haga K and Huang H H 2019 High-pressure oxidative leaching and iodide leaching followed by selective precipitation for recovery of base and precious metals from waste printed circuit boards ash *Met. (Basel)* **9** 3

[4] Sahajwalla V and Hossain R 2020 The science of microrecycling: a review of selective synthesis of materials from electronic waste *Mater. Today Sustain.* **9** 100040

[5] Silva W C, de Souza Corrêa R, da Silva C S M, Afonso J C, da Silva R S, Vianna C A and Mantovano J L 2018 Recovery of base metals, silicon and fluoride ions from mobile phone printed circuit boards after leaching with hydrogen fluoride and hydrogen peroxide mixtures *Waste Manag.* **78** 781–8

[6] Suganuma K 2001 Advances in lead-free electronics soldering *Curr. Opin. Solid State Mater. Sci.* **5** 55–64

[7] Stenvall E, Tostar S, Boldizar A, Foreman M R S J and Möller K 2013 An analysis of the composition and metal contamination of plastics from waste electrical and electronic equipment (WEEE) *Waste Manag.* **33** 915–22

[8] Forti V, Balde C P, Kuehr R and Bel G 2020 *The Global E-Waste Monitor Quantities, Flows and the Circular Economy Potential* (Bonn, Geneva and Rotterdam: United Nations University/United Nations Institute for Training and Research, International Telecommunication Union, and International Solid Waste Association, 2020)

[9] Sahan M, Kucuker M A, Demirel B, Kuchta K and Hursthouse A 2019 Determination of metal content of waste mobile phones and estimation of their recovery potential in Turkey *Int. J. Environ. Res. Public Health* **16** 5

[10] Hagelüken C and Corti C W 2010 Recycling of gold from electronics: cost-effective use through 'design for recycling' *Gold Bull.* **43** 209–20

[11] Charles R G, Douglas P, Hallin I L, Matthews I and Liversage G 2017 An investigation of trends in precious metal and copper content of RAM modules in WEEE: Implications for long term recycling potential *Waste Manag.* **60** 505–20

[12] Holuszko M E, Kumar A and Espinosa D C R 2021 *Electronic waste : recycling and reprocessing for a sustainable future* (New York: Wiley)

[13] Syed S 2012 Recovery of gold from secondary sources-a review *Hydrometallurgy* **115–116** 30–51

[14] Cecchi T 2015 Chimica, preziosa chimica! Estraiamo oro dai rifiuti RAEE! *Profiles* ed L Cardellini 3 (Ancona, Italy: Università Politecnica delle Marche)

[15] Alzate A, López M E and Serna C 2016 Recovery of gold from waste electrical and electronic equipment (WEEE) using ammonium persulfate *Waste Manag.* **57** 113–20

[16] Alzate A, López E, Serna C and Gonzalez O 2017 Gold recovery from printed circuit boards by selective breaking of internal metallic bonds using activated persulfate solutions *J. Clean. Prod.* **166** 1102–12

[17] Syed S 2006 A green technology for recovery of gold from non-metallic secondary sources *Hydrometallurgy* **82** 48–53

[18] Lu Y and Xu Z 2017 Recycling non-leaching gold from gold-plated memory cards: parameters optimization, experimental verification, and mechanism analysis *J. Clean. Prod.* **162** 1518–26

[19] Barbieri L, Giovanardi R, Lancellotti I and Michelazzi M 2010 A new environmentally friendly process for the recovery of gold from electronic waste *Environ. Chem. Lett.* **8** 171–8

[20] Zhang X, Zhang C, Zheng F, Ma E, Wang R, Bai J, Yuan W and Wang J 2020 Alkaline electrochemical leaching of Sn and Pb from the surface of waste printed circuit board and the stripping of gold by methanesulfonic acid *Environ. Prog. Sustain. Energy* **39** 1–8

[21] Wang Z, Guo S and Ye C 2016 Leaching of Copper from Metal Powders Mechanically Separated from Waste Printed Circuit Boards in Chloride Media Using Hydrogen Peroxide as Oxidant *Procedia Environ. Sci.* **31** 917–24

[22] Bozell J J and Petersen G R 2010 technology development for the production of biobased products from biorefinery carbohydrates-the us department of energy's 'top 10' revisited *Green Chem.* **12** 539–54

[23] Cecchi T and De Carolis C 2021 Biobased Products from Food Sector Waste : Bioplastics, Biocomposites, and Biocascading 1st ed. 2021 Springer

[24] Smithers G W 2008 Whey and whey proteins-From 'gutter-to-gold' *Int. Dairy J.* **18** 695–704

[25] Chen T, Kitada A, Fukami K and Murase K 2019 Determination of stability constants of copper(II)–lactate complexes in Cu_2O electrodeposition baths by UV–vis absorption spectra factor analysis *J. Electrochem. Soc.* **166** D761–7

[26] Lee H J, Lee H and Lee C 2014 Degradation of diclofenac and carbamazepine by the copper(II)-catalyzed dark and photo-assisted Fenton-like systems *Chem. Eng. J.* **245** 258–64

[27] Chumakov A, Batalova V and Slizhov Y 2016 Electro-Fenton-like reactions of transition metal ions with electrogenerated hydrogen peroxide *AIP Conf. Proc.* **1772** 040004

[28] Kim K, Lee K, So S, Cho S, Lee M, You K, Moon J and Song T 2018 Fenton-like reaction between copper ions and hydrogen peroxide for high removal rate of tungsten in chemical mechanical planarization *ECS J. Solid State Sci. Technol.* **7** P91–5

[29] Vogel A I 1945 Vogel Textbook of Quantitative Analysis *Longman Scientific & Technical* (*Quantitative Chemical Analysis*) ed G H Jefferey *et al* 5th edn (Harlow: Longman) Green and Co. Ltd

[30] McKenzie D R 1978 Gold black and gold cermet absorbing surfaces *Gold Bull.* **11** 49–53

[31] Hovington P, Drouin D and Gauvin R 1997 CASINO: a new Monte Carlo code in C language for electron beam interaction - part I: description of the program *Scanning* **19** 1–14

[32] Achilli E, Vertova A, Visibile A, Locatelli C, Minguzzi A, Rondinini S and Ghigna P 2017 Structure and stability of a copper(II) lactate complex in alkaline solution: a case study by energy-dispersive x-ray absorption spectroscopy *Inorg. Chem.* **56** 6982–9

[33] Mech K, Bisztyga-Szklarz M and Szaciłowski K 2020 Brief Insights into Cu_2O Electrodeposition: Detailed Progressive Voltammetric and Electrogravimetric Analysis of a Copper Lactate System *J. Electrochem. Soc.* **167** 042504

[34] Deng D, Cheng Y, Jin Y, Qi T and Xiao F 2012 Antioxidative effect of lactic acid-stabilized copper nanoparticles prepared in aqueous solution *J. Mater. Chem.* **22** 23989–95

[35] Noriega R, Rivnay J, Vandewal K, Koch F, Stingelin N, Smith P, Toney M and Salleo A 2013 A general relationship between disorder, aggregation and charge transport in conjugated polymers *Nat. Mater.* **12** 1038–44

[36] Bishara H, Lee S, Brink T, Ghidelli M and Dehm G 2021 Understanding grain boundary electrical resistivity in Cu: the effect of boundary structure *ACS nano* **15** 16607–15

[37] Reiss G, Vancea J and Hoffmann H 1986 Grain-boundary resistance in polycrystalline metals *Phys. Rev. Lett.* **56** 2100

[38] Gall D 2020 The search for the most conductive metal for narrow interconnect lines *J. Appl. Phys.* **127** 050901